Journal Name

ARTICLE

Interactions between Circulating Nanoengineered Polymer Particles and Extracellular Matrix Components *In Vitro*†

Received 00th January 20xx,
Accepted 00th January 20xx

DOI: 10.1039/x0xx00000x

www.rsc.org/

Julia A. Braunger,[a,‡] Mattias Björnmalm,[a,‡] Nathan A. Isles,[a] Jiwei Cui,[a] Timothy M. A. Henderson,[b] Andrea J. O'Connor,[b] and Frank Caruso[a,*]

The extracellular matrix (ECM) that surrounds cells *in vivo* represents a biological barrier for nanomaterials in biomedicine. Herein, we present a system for investigating the interactions between circulating polymer particles and ECM components *in vitro* using a commercially available flow-based device. We use this system to show how material-dependent interactions of two different particle types—one assembled using poly(ethylene glycol) (PEG) and one prepared using poly(methacrylic acid) (PMA)—affect their interactions with basement membrane extracts during *in vitro* circulation, with PEG particles remaining in circulation longer than PMA particles. Further, by comparing macroporous hyaluronic acid gel constructs (typically used for tissue engineering) with basement membrane extracts, we show that scaffold-effects (porosity and surface chemistry) impact on circulation time *in vitro*. The presented system is simple and modular, and can be used to rapidly screen fundamental interactions of engineered particles with biologically relevant microenvironments under flow-conditions.

Introduction

Nanoengineered polymer particles are of interest for a range of biomedical applications, including vaccination, bioreactions, and drug delivery.[1–4] Successful drug delivery with particles is a complex challenge; e.g., intravenously administered particles targeting tumour tissue have to negotiate multiple biological barriers.[5] These include evasion of systemic clearance and extravasation, transport through the interstitial space and eventually internalization into target cells.[6–10] Some of these barriers have been extensively studied and particle design parameters aimed toward overcoming them have started to emerge.[5,11–13] One important barrier that is receiving increasing attention is the local environment of the diseased tissue, such as the tumour microenvironment and associated interstitium.[14]

The tumour microenvironment is characterized by abnormal vasculature and tissue/cellular organization causing phenomena such as "vascular bursts" and the "enhanced permeability and retention effect" that allow macromolecules and particles (approximately 10 to 500 nm in diameter) to escape the vascular bed and accumulate inside the interstitial space.[15–18] Blood vessels are supported by a specialized form of the ECM, the basement membrane, which like the ECM contain molecules such as collagen, proteoglycans, and hyaluronic acid (HA), among many others.[19–21] Understanding how therapeutics interact with these biological environments is therefore important for biomedical applications such as drug delivery.[22–24]

Previous studies have shown that extracellular matrix gels can filter or trap polystyrene particles,[25] and that this effect can be modulated through ion-specific effects.[26] Tumour spheroids, made of aggregated tumour cells, have also been used to investigate the shape- and size-dependent penetration of nanoparticles.[27–29] Flow-based devices (e.g., macro- and microfluidic devices)[30,31] can aid in these studies, as they can recapitulate the flow environment present in virtually all soft tissues.[32] These types of devices have been used to investigate gold nanoparticle penetration into tumour spheroids and collagen gels under dynamic culture conditions.[33,34] These studies show the importance of studying particle-ECM effects, however, the use of either polystyrene beads or rigid gold particles may not be representative of "softer" particle types; the latter being an emerging class of particles being explored for nanomedicine.[1–4,13] Furthermore, most studies focus on bio-particle interactions under static conditions (e.g., using multiwell plates), with relatively few studies on fundamental bio-nano interactions of particles in dynamic *in vitro* settings (e.g., under flow or in circulation).

Herein, we report a strategy for the investigation of particle-ECM interactions using a commercially available 3D bioreactor (3DKUBE, Kiyatec) coupled with an *in vitro* circulation system (Fig. 1). We fill the bioreactors with either basement membrane extracts or hyaluronic acid-based

[a] *ARC Centre of Excellence in Convergent Bio-Nano Science and Technology, and the Department of Chemical and Biomolecular Engineering, The University of Melbourne, Parkville, Victoria 3010, Australia. *E-mail: fcaruso@unimelb.edu.au*
[b] *Department of Chemical and Biomolecular Engineering, The University of Melbourne, Parkville, Victoria 3010, Australia.*

† Electronic Supplementary Information (ESI) available: Supplementary figures and experimental details. See DOI: 10.1039/x0xx00000x

‡ These authors contributed equally.

cryogels (tissue engineering scaffolds described previously),[35,36] connect the bioreactors in-line to the circulation system, inject particles into the circulation, and study the particle interactions with the gels using flow cytometry and confocal laser scanning microscopy. We study and compare two types of soft polymer particles—poly(ethylene glycol) (PEG) and poly(methacrylic acid) (PMA) based particles—and show that material-dependent interactions affect particle removal from circulation in both the gel and scaffold systems.

Materials and methods

Materials. Sodium hyaluronate (HA, M_W 60 kDa) was purchased from Lifecore Biomedical (Minnesota, USA). ECM gel from Engelbreth-Holm-Swarm murine sarcoma (Matrigel matrix, 9.24 mg ml^{-1} protein), 1-ethyl-3-(3-dimethylaminopropyl)carbodiimide (EDC), *N*-hydroxysuccinimide (NHS), Rhodamine B, dithiothreitol (DTT), and phosphate buffered saline (PBS) were purchased from Sigma-Aldrich. 8-arm-PEG-NH_2 (40 kDa) and 8-arm-PEG-NHS (10 kDa) with a hexaglycerol core structure were purchased from JenKem Technology USA Inc. (China). Poly(methacrylic acid, sodium salt) (PMA, M_W 15 kDa, 30 wt.% solution in water) was obtained from Polysciences, Inc. (USA). Pyridine dithioethylamine (PDA) was purchased from Shanghai Speed Chemical Co. Ltd. (China). Alexa Fluor 488 carboxylic acid, succinimidyl ester (AF488-NHS) and Alexa Fluor 488 C5 maleimide (AF488-maleimide) was obtained from Life Technologies (Australia). The Kiyatec 3DKUBE bioreactors/perfusion chambers (Sigma product number: Z692026) and the 3D Biotek 3D insert polystyrene scaffolds (for 96-well plate, fibre diameter: 150 µm, pore size: 200 µm; Sigma product number: Z724300) were purchased through Sigma-Aldrich. Peristaltic pump tubing (PharMed, ID 0.76 mm) was purchased from Ismatec (Germany). µ-Slide Chemotaxis3D was obtained from Ibidi (Germany). Anti-collagen IV antibody (reference number: ab19808) was purchased from abcam. Goat anti-rabbit IgG (H+L) secondary antibody and Alexa Fluor 488 conjugate were purchased from Life Technologies. All water used in the experiments was purified water with a resistivity of 18.2 MΩ cm (obtained from an inline Millipore RiOs/Origin water purification system).

Particle engineering. Both particle types were prepared using mesoporous silica replication[37] and the same batch of mesoporous silica templates were used for the preparation of both particle types (Fig. S1). The strategy for preparing PEG replica particles has been described previously.[38,39] Briefly, MS particles (500 ± 65 nm in diameter)[39] were infiltrated with branched PEG polymers and then cross-linked based on NHS-chemistry (Fig. S2). PMA replica particles were fabricated using thiol-disulphide exchange cross-linking (Fig. S3).[40–42] Both particle types were fluorescently labelled with Alexa Fluor 488 (AF488) before the silica templates were removed with buffered hydrofluoric acid. Particles were characterized using optical microscopy, fluorescence microscopy, electron microscopy, microelectrophoresis (to calculate zeta (ζ)-potentials), and flow cytometry. Additional characterization

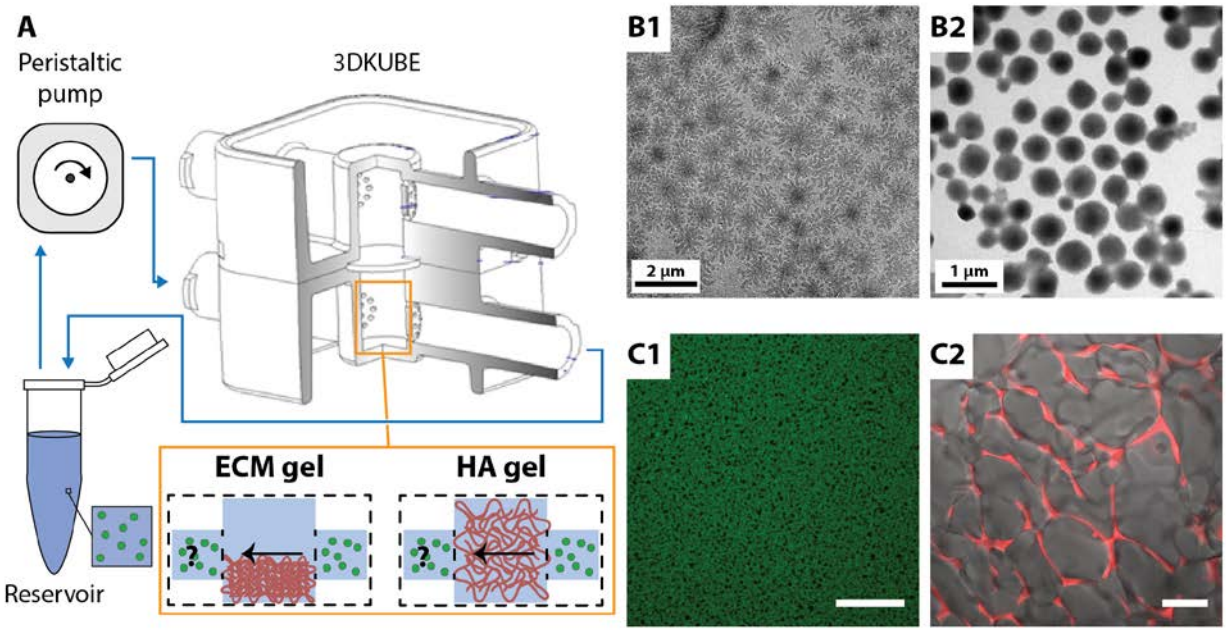

Fig. 1. Design of flow system for evaluating interactions of particles with ECM components using a 3DKUBE flow chamber. (A) Schematic of the flow system. The inner chamber of the 3DKUBE is 6 mm in diameter and can hold 250 µL of liquid (see Fig. S4 for additional details). (B) Transmission electron microscopy images of PEG (B1) and PMA (B2) replica particles. Note that these images are of dried particles in vacuum. (C1) Fluorescence microscopy image of anti-collagen IV-labeled ECM gel. The green color is the gel and the black areas are the pores. (C2) Overlay of bright field and fluorescence microscopy image of the Rhodamine B-labeled HA cryogel. Scale bars in C1 and C2 are 50 µm.

(including atomic force microscopy and super-resolution microscopy) for these particle systems has been previously reported.[37–42]

Gel fabrication and characterization. Macroporous HA cryogels were prepared according to our previously published method by cryogelation with EDC-mediated zero-length crosslinking in custom-made glass and acrylic molds.[35] HA gels were labelled with Rhodamine B through rehydration. Matrigel matrix, used as a model ECM gel, was characterized based on a previously published method.[43] Briefly, fixed ECM gels were stained with a primary antibody (anti-collagen IV antibody) followed by a secondary antibody (goat-anti-rabbit AF488 IgG). Images of both gels were taken using a Nikon A1R+ laser scanning confocal microscope.

Preparation of 3DKUBE chambers with ECM gel. 60 µl of ECM gel was transferred into a chamber of a 3DKUBE bioreactor (Fig. S4) using a chilled (4 °C) pipette tip. Four polystyrene insert scaffolds (3D Insert-PS) were immersed into the liquid ECM gel in each chamber to confer additional stability to the gel for the flow experiments. The 3DKUBE chambers filled with ECM gels were placed in a humidified box and incubated at 37 °C for 1 h to allow for gelation.

Preparation of 3DKUBE chambers filled with cryogel scaffold. Four HA gel discs were cut using a biopsy punch (6 mm diameter), and placed on top of each other into each 3DKUBE chamber.

Flow setup. The flow setup consisted of a 1.7 mL microcentrifuge tube as a reservoir, a flow chamber (the 3DKUBE), a peristaltic pump, and tubing (Fig. 1A and Fig. S5). We have previously used the 3DKUBE for the engineering of particles in a similar setup.[44] The 3DKUBE chamber containing the ECM gel or HA cryogel scaffold was completely filled with PBS and the unit was connected to the tubing in a drop-by-drop fashion to avoid introduction of air bubbles. 5×10^8 particles in 600 µL PBS were prepared and samples were taken to determine the initial particle concentration, taking the dilution of the fluidic system into account. The particle concentration used was based on what has previously been reported for *in vivo* studies in mice.[39] The total flow volume in the setup was 1.2 mL, which corresponds to the blood volume of a mouse (20 g body weight).[45] Samples were taken at designated time points and analysed via flow cytometry (Apogee A50 Micro) to follow the particle distribution over time in relation to initial particle concentration. Flow experiments were performed in triplicate and the data is presented as the mean with standard deviation. After completion, the gels and scaffolds were removed from the chamber and imaged using an Olympus IX71 fluorescence microscope and a Nikon A1R+ laser scanning confocal microscope.

Additional experimental information can be found in the ESI.†

Results and discussion

As model particle systems we used fluorescently labelled PEG and PMA replica particles. While the PEG particles are low-fouling and show low association to human blood cells and prolonged circulation times *in vivo* in mice,[39] the PMA particles interact extensively with cells and can be considered high-fouling.[46] TEM images show rather dense PMA particles and less dense PEG particles (Fig. 1B1-B2). The ζ-potentials were determined to be –4 ± 2 mV and –38 ± 5 mV for the PEG and PMA replica particles, respectively.

The ECM gel used was Matrigel matrix purified from Engelbreth–Holm–Swarm sarcoma of mice, a gel widely used as a model system for native basal lamina.[47–49] We characterized the ECM gel by staining with collagen IV, which is one of the main components of the basement membrane.[19] We found a dense network showing pores of a few micrometres in size (Fig. 1C1), in agreement with others.[43] For visualization of the HA gels we used bright field, fluorescence and confocal microscopy, which revealed a macroporous structure with pores between 40 and 80 µm in the HA gels (Fig. 1C2 and 2), as expected.[35]

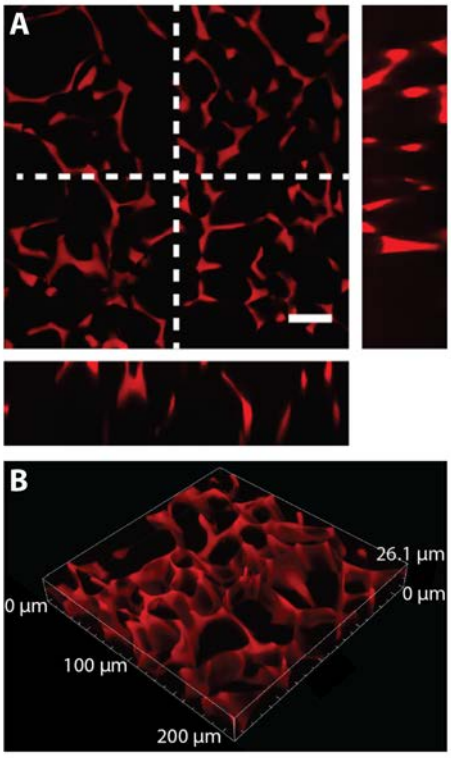

Fig. 2. (A) Cross-sections of Rhodamine B-labeled HA cryogel with connected pores. Scale bar is 50 µm. (B) Volume rendering of Rhodamine B-labeled HA cryogel.

The flow devices were assembled and reservoirs containing 5×10^8 particles were prepared. Before the particle reservoir was connected to the flow system, a sample to determine the initial particle concentration was taken. Using a flowrate of 70 µL min^{-1}, samples were taken at designated time points and the particle concentration was determined using flow cytometry.

After assembling and characterizing the particles, gels, and the flow-based system we investigated how the particles

interacted with model ECM gels. The bioreactor was filled half-full with the ECM gel, enabling the particles to interact with the ECM gel by traversing across its surface and by potentially being transported into the pores of the gel. Fig. 3A shows the particle concentration in circulation monitored over time.

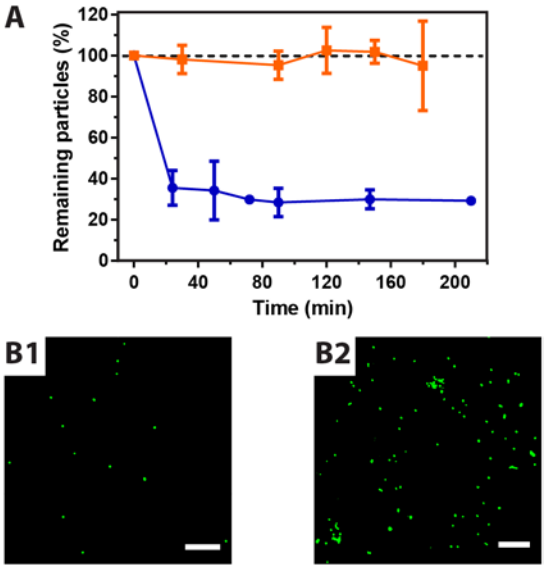

Fig. 3. (A) Particle circulation in the flow system containing the ECM gel. (A) Change in concentration of PEG (orange squares) and PMA (blue circles) replica particles over time, as monitored via flow cytometry. (B) Fluorescence microscopy images of the surface of the ECM gels after circulation experiments, showing adsorbed (B1) PEG and (B2) PMA particles. Scale bars are 10 µm. Some error bars are not visible as they are within the size of the data points.

The PEG particles remained in circulation and after 3 h the particle concentration remained high, around 95 ± 20% of the initial concentration. In contrast, the PMA particles were removed relatively quickly from circulation with only 36 ± 8% remaining after 20 min. The remaining particles were then removed more slowly and after 3.5 h 29 ± 0.2% of the initial particle concentration remained. Considering that both particle systems were prepared through mesoporous silica templating using templates from the same batch, are of approximately the same size, and show negligible material-specific adsorption during circulation in the empty flow setup (Fig. S6), the differences in particle concentration observed can be attributed to material-specific interactions and binding to the ECM gel.

To further investigate the fate of particles removed from circulation, the fluidic system was flushed with PBS to remove unbound and loosely attached particles, the bioreactor was disassembled and the ECM gel surface was imaged using fluorescence microscopy (Fig. 3B). For the PEG particles, we found only minor surface attachment (Fig. 3B1), whereas the PMA particles were found to be adsorbed to a greater extent (Fig. 3B2), in agreement with the results obtained from flow cytometry. These microscopy studies also showed that there was limited particle penetration into the gels, which is not unexpected as the pore size of these gels was found to be small (a few micrometres in diameter, Fig. 1C1). Although this is larger than the particle size (fabricated from templates 500 ± 65 nm in diameter) the dense structure of the ECM gel causes high fluidic resistance and favours liquid flow around the ECM gel, instead of through it (Fig. 1A).

The observed differences in removal from circulation can be attributed to the low- and high-fouling nature of the PEG[39] and PMA[46] replica particles, respectively. An important underlying factor is the neutral and negative surface charge of the particles: –4 ± 2 and –38 ± 5 mV for the PEG and PMA replica particles, respectively. The negative surface charge of the PMA replica particles can induce attachment to positively charged 'patches' of the ECM gel,[25] which would contribute to the observed particle loss from circulation.

After investigating how model ECM gels interact with engineered particles in circulation we changed the ECM gel to a tissue engineering construct, namely a HA-based cryogel. Tissue engineering constructs are of interest for fundamental science (as biomimetics) and for biomedical applications.[36] By studying how particles and scaffolds interact, bio-nano interactions in engineered biomimetic environments can be probed. This can facilitate the fundamental understanding of tissue engineering scaffolds and of engineered particles. Herein, we used a HA-based macroporous cryogel (Fig. 2).[35] The cryogels were placed into the bioreactors and exposed to particles in circulation using our flow-based system. The concentration of circulating particles was then determined over time using flow cytometry (Fig. 4).

The concentrations of both PEG and PMA particles in circulation were found to decrease over time when the cryogels were used, which is in contrast to the ECM gel experiments. But, interestingly, after 2 h, 45 ± 8% of the PMA replica particles remained in circulation while for the PEG replica particles this increased to 66 ± 1% (Fig. 4A). This difference in the amount of remaining circulating particles is present already after 20 min, and stabilizes over the 2 h investigated.

PEG and PMA particles display different trends in the two gel systems. While PEG particles are removed quicker from circulation for HA gels (66 ± 1% after 2 h) compared to ECM gels (95 ± 20% after 3 h) the opposite was observed for PMA particles (45 ± 8% after 2 h for HA gels and 29 ± 0.2% after 3.5 h for ECM gels, respectively). The HA cryogels have a negative surface charge (while the ECM gels have positively charged 'patches'),[25] which can, in part, explain the observed difference in loss from circulation for PMA particles (with a negative surface charge) when comparing the two gel systems.

After the flow experiments, we removed the HA gels from the chambers and imaged them using confocal microscopy (Fig. 4B). Both PEG and PMA replica particles were found to have attached to the HA gels. Therefore, similar to the interaction with the ECM gel, the observed particle loss from circulation is (at least partly) due to particles attaching to the matrix. HA is a well-known low-fouling material[36,50,51] but the

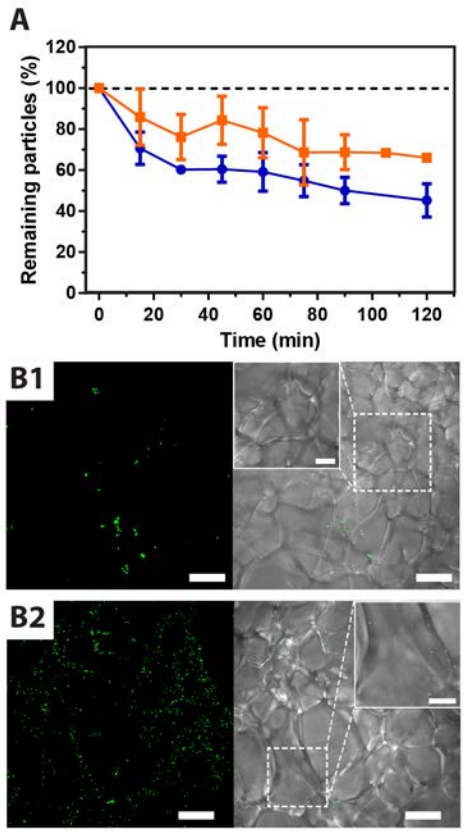

Fig. 4. Particle circulation in the flow system containing the HA cryogel. (A) Change in concentration of PEG (orange squares) and PMA (blue circles) replica particles over time, as monitored via flow cytometry. (B) Maximum intensity projections of confocal (fluorescence) z-stacks and bright-field microscopy after circulation experiments showing adsorbed (B1) PEG and (B2) PMA particles. Scale bars are 50 µm for full images and 20 µm for insets. Some error bars are not visible as they are within the size of the data points.

macroporous structure of the HA gels provide a large accessible surface area. However, more PMA particles were still visibly bound to the HA gel matrix compared to the PEG particles (Fig. 4B1-B2).

The HA cryogels used are highly macroporous (pores around 40-80 µm, Fig. 1C2 and Fig. 2) in comparison to the ECM gels (Fig. 1C1), which suggests particles were able to more easily enter the cryogels. The open porous structure of the HA cryogels also suggests that particles may not be attached to the surfaces to be removed from circulation, but just trapped inside the cryogels. To investigate this, we flushed the system briefly after the circulation experiments and recorded a time series (Video S1). The video shows that most of the PEG particles were mobile but trapped within the porous HA gel structure and similar behaviour was observed for the PMA particles. Consequently, the loss of particles during circulation can be attributed, on the one hand, to material-specific interactions, which in this setup caused around a 20% difference in circulation loss when comparing PMA and PEG replica particles. On the other hand, a subpopulation of particles is mobile but trapped (or at least retarded) inside the macroporous HA cryogels.

To investigate the effects of initial particle concentration (e.g., to study possible saturation effects), we increased the initial particle number by 50% (from 5 to 7.5 × 10^8 particles per experiment) and studied the effect on particle circulation behaviour (Fig. 5A). For PMA particles we observed similar behaviour compared to the standard initial particle number. For the PEG particles, an increase in variability was observed, although the overall trend remained similar compared to the standard initial particle number. This indicates that saturation effects were low in the system.

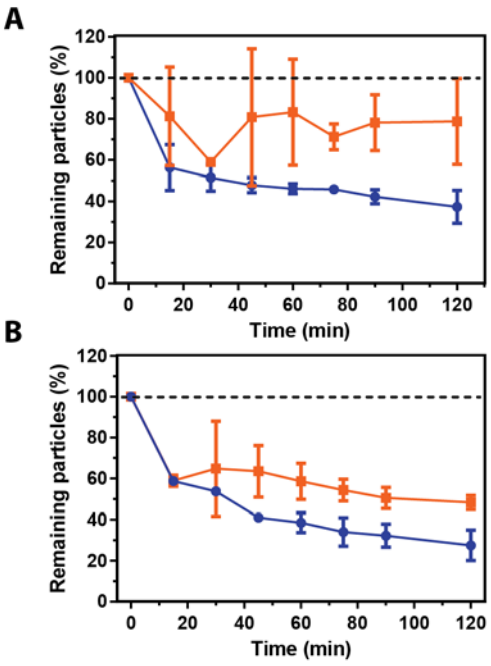

Fig. 5. Change in concentration of PEG (orange squares) and PMA (blue circles) replica particles during circulation in flow systems containing HA gels, as monitored via flow cytometry. Effect of increasing initial particle number (A) or flow rate (B) by 50%. Some error bars are not visible as they are within the size of the data points.

To investigate the effect of flow rate and particle velocity on scaffold-particle interactions we increased the flow rate by 50% (from 70 to 105 µL min^{-1}) and measured the particle number in circulation over time (Fig. 5B). Both concentration profiles showed that the particles were removed to a greater extent from circulation compared to circulation experiments performed at the standard flow rate. Approximately 48 ± 3% of the initial PEG particle concentration remained in circulation after 2 h at the higher flow rate (Fig. 5B) compared to 66 ± 1% for the standard flow rate (Fig. 4A). Similarly, 28 ± 7% of the PMA particles remained in circulation after 2 h at the increased flow rate (Fig. 5B) compared to 45 ± 8% under standard flow conditions (Fig. 4A). Interestingly, a trend consistent with the experiments performed at a standard flow

rate was observed, where material-specific differences between PEG and PMA particle concentration of around 20% was established after around 45 min, indicating that the greater removal of particles from circulation at an increased flow rate is mainly due to particles being trapped inside the porous network of the cryogel. The higher flow rate means particles circulate through the system more quickly, thus increasing the number of times particles interact with the gel. For example, if the particles circulate the system twice per minute instead of once per minute, particles that remain in circulation will flow past the gels ten times instead of five times during a five-minute period, which may increase the possibility of entrapment inside the porous networks of the cryogels. The hydrodynamic shear forces within the gels would also be greater, potentially leading to particles coming into closer contact with the gel surfaces and having a greater probability of interacting with the pore walls.

Summary and conclusions

This study presents the use of a flow-based system for investigating fundamental interactions between circulating soft polymer particles and biological or biomimetic environments. We used two types of particles (made from the same template) to examine material-based effects, and two types of scaffolds to probe scaffold-based effects. We investigated material-dependent interactions of PMA and PEG replica particles, and found that the latter exhibit extended circulation times in the *in vitro* system when using basal lamina extract gels, which corresponds well with *in vivo* results in mice.[39] Additionally, we also investigated scaffold-effects by comparing these results to those obtained when using a HA-based tissue engineering construct instead of the ECM gel. We found that both particle types were removed from circulation because of both material-specific interactions with the HA gel, which was more pronounced for the PMA particles, and physical entrapment leading to particles being mobile but trapped within the macroporous HA cryogels. Further, by changing the initial particle concentrations we showed that saturation effects were low in the system, and by changing the flow rates we showed that particle velocity effects increased the rate of removal from circulation.

Although our circulation setup is far from the complexity encountered *in vivo*, it allows for quick assessment of basic barrier functions of ECM components and biomimetic scaffolds *in vitro*, enabling simple and rapid investigation of fundamental particle-bio interactions. For example, it has previously been shown that particle morphology affects bio-interactions under flow,[52,53] and this is part of our future studies using our circulation system. The modular approach also enables the complexity of the system to be tuned, facilitating systematic approaches based around convergent science.[54] For example, multiple bioreactors could be assembled in series or in parallel, similar to the concept of using multiple, continuously perfused microchambers in microfluidic devices to create "organs-on-chips".[55,56] The tissue engineering scaffolds used here can support cell cultures,[35] and we have performed initial tests using 3D cell cultures inside the bioreactors. Although this introduces additional complexity (sterile conditions and incubation required) this could enable new types of bio-nano and particle-scaffold interactions to be investigated under physiologically relevant flow conditions. Taken together, these results demonstrate a simple and rapid way of investigating fundamental bio-interactions of circulating soft polymer particles *in vitro*.

Acknowledgements

This research was conducted and funded by the Australian Research Council (ARC) Centre of Excellence in Convergent Bio-Nano Science and Technology (Project CE140100036) and funded by the ARC under the Australian Laureate Fellowship (FL120100030) scheme. This work was performed in part at the Materials Characterisation and Fabrication Platform (MCFP) at the University of Melbourne and the Victorian Node of the Australian National Fabrication Facility (ANFF).

Notes and references

1 M. Elsabahy, G. S. Heo, S.-M. Lim, G. Sun and K. L. Wooley, *Chem. Rev.*, 2015, **115**, 10967–11011.
2 D. J. Irvine, M. C. Hanson, K. Rakhra and T. Tokatlian, *Chem. Rev.*, 2015, **115**, 11109–11146.
3 J. Gaitzsch, X. Huang and B. Voit, *Chem. Rev.*, 2016, **116**, 1053–1093.
4 J. Cui, J. J. Richardson, M. Björnmalm, M. Faria and F. Caruso, *Acc. Chem. Res.*, 2016, **49**, 1139–1148.
5 E. Blanco, H. Shen and M. Ferrari, *Nat. Biotechnol.*, 2015, **33**, 941–951.
6 S. Wilhelm, A. J. Tavares, Q. Dai, S. Ohta, J. Audet, H. F. Dvorak and W. C. W. Chan, *Nat. Rev. Mater.*, 2016, **1**, 16014.
7 M. W. Tibbitt, J. E. Dahlman and R. Langer, *J. Am. Chem. Soc.*, 2016, **138**, 704–717.
8 Y. Yan, M. Björnmalm and F. Caruso, *Chem. Mater.*, 2014, **26**, 452–460.
9 A. E. Nel, L. Mädler, D. Velegol, T. Xia, E. M. V Hoek, P. Somasundaran, F. Klaessig, V. Castranova and M. Thompson, *Nat. Mater.*, 2009, **8**, 543–557.
10 M. Kanapathipillai, A. Brock and D. E. Ingber, *Adv. Drug Deliv. Rev.*, 2014, **79–80**, 107–118.
11 R. A. Petros and J. M. DeSimone, *Nat. Rev. Drug Discov.*, 2010, **9**, 615–627.
12 A. Albanese, P. S. Tang and W. C. W. Chan, *Annu. Rev. Biomed. Eng.*, 2012, **14**, 1–16.
13 C. J. Cheng, G. T. Tietjen, J. K. Saucier-Sawyer and W. M. Saltzman, *Nat. Rev. Drug Discov.*, 2015, **14**, 239–247.
14 V. P. Chauhan and R. K. Jain, *Nat. Mater.*, 2013, **12**, 958–962.
15 V. Torchilin, *Adv. Drug Deliv. Rev.*, 2011, **63**, 131–135.
16 H. Maeda, *Adv. Drug Deliv. Rev.*, 2015, **91**, 3–6.
17 F.-R. E. Curry, *Nat. Nanotechnol.*, 2016, **11**, 494–496.
18 Y. Matsumoto, J. W. Nichols, K. Toh, T. Nomoto, H. Cabral,

Y. Miura, R. J. Christie, N. Yamada, T. Ogura, M. R. Kano, Y. Matsumura, N. Nishiyama, T. Yamasoba, Y. H. Bae and K. Kataoka, *Nat. Nanotechnol.*, 2016, **11**, 533–538.
19 R. Kalluri, *Nat. Rev. Cancer*, 2003, **3**, 422–433.
20 J. K. Mouw, G. Ou and V. M. Weaver, *Nat. Rev. Mol. Cell Biol.*, 2014, **15**, 771–785.
21 P. Baluk, S. Morikawa, A. Haskell, M. Mancuso and D. M. McDonald, *Am. J. Pathol.*, 2003, **163**, 1801–1815.
22 P. A. Netti, D. A. Berk, M. A. Swartz, A. J. Grodzinsky and R. K. Jain, *Cancer Res.*, 2000, **60**, 2497–503.
23 S. Ramanujan, A. Pluen, T. D. McKee, E. B. Brown, Y. Boucher and R. K. Jain, *Biophys. J.*, 2002, **83**, 1650–1660.
24 K. Yokoi, M. Kojic, M. Milosevic, T. Tanei, M. Ferrari and A. Ziemys, *Cancer Res.*, 2014, **74**, 4239–4246.
25 O. Lieleg, R. M. Baumgärtel and A. R. Bausch, *Biophys. J.*, 2009, **97**, 1569–1577.
26 F. Arends, R. Baumgärtel and O. Lieleg, *Langmuir*, 2013, **29**, 15965–15973.
27 S. Huo, H. Ma, K. Huang, J. Liu, T. Wei, S. Jin, J. Zhang, S. He and X. J. Liang, *Cancer Res.*, 2013, **73**, 319–330.
28 K. Huang, H. Ma, J. Liu, S. Huo, A. Kumar, T. Wei, X. Zhang, S. Jin, Y. Gan, P. C. Wang, S. He, X. Zhang and X.-J. Liang, *ACS Nano*, 2012, **6**, 4483–4493.
29 R. Agarwal, P. Jurney, M. Raythatha, V. Singh, S. V. Sreenivasan, L. Shi and K. Roy, *Adv. Healthc. Mater.*, 2015, **4**, 2269–2280.
30 P. M. Valencia, O. C. Farokhzad, R. Karnik and R. Langer, *Nat. Nanotechnol.*, 2012, **7**, 623–629.
31 M. Björnmalm, Y. Yan and F. Caruso, *J. Control. Release*, 2014, **190**, 139–149.
32 M. A. Swartz and M. E. Fleury, *Annu. Rev. Biomed. Eng.*, 2007, **9**, 229–256.
33 A. Albanese, A. K. Lam, E. A. Sykes, J. V Rocheleau and W. C. W. Chan, *Nat. Commun.*, 2013, **4**, 2718.
34 V. Raeesi and W. C. W. Chan, *Nanoscale*, 2016, **8**, 12524–12530.
35 T. M. A. Henderson, K. Ladewig, D. N. Haylock, K. M. McLean and A. J. O'Connor, *J. Biomater. Sci. Polym. Ed.*, 2015, **26**, 881–897.
36 T. M. A. Henderson, K. Ladewig, D. N. Haylock, K. M. McLean and A. J. O'Connor, *J. Mater. Chem. B*, 2013, **1**, 2682.
37 M. Björnmalm, J. Cui, N. Bertleff-Zieschang, D. Song, M. Faria, M. A. Rahim and F. Caruso, *Chem. Mater.*, 2016, DOI: 10.1021/acs.chemmater.6b02848.
38 J. Cui, M. Björnmalm, K. Liang, C. Xu, J. P. Best, X. Zhang and F. Caruso, *Adv. Mater.*, 2014, **26**, 7295–7299.
39 J. Cui, R. De Rose, K. Alt, S. Alcantara, B. M. Paterson, K. Liang, M. Hu, J. J. Richardson, Y. Yan, C. M. Jeffery, R. I. Price, K. Peter, C. E. Hagemeyer, P. S. Donnelly, S. J. Kent and F. Caruso, *ACS Nano*, 2015, **9**, 1571–1580.
40 J. Cui, R. De Rose, J. P. Best, A. P. R. Johnston, S. Alcantara, K. Liang, G. K. Such, S. J. Kent and F. Caruso, *Adv. Mater.*, 2013, **25**, 3468–3472.
41 J. P. Best, J. Cui, M. Müllner and F. Caruso, *Langmuir*, 2013, **29**, 9824–9831.
42 J. Cui, M. Faria, M. Björnmalm, Y. Ju, T. Suma, S. T. Gunawan, J. J. Richardson, H. Heidari, S. Bals, E. J. Crampin and F. Caruso, *Langmuir*, 2016, doi: 10.1021/acs.langmuir.6b01634.
43 F. Arends, C. Nowald, K. Pflieger, K. Boettcher, S. Zahler and O. Lieleg, *PLoS One*, 2015, **10**, e0118090.
44 J. J. Richardson, M. Björnmalm, S. T. Gunawan, J. Guo, K. Liang, B. Tardy, S. Sekiguchi, K. F. Noi, J. Cui, H. Ejima and F. Caruso, *Nanoscale*, 2014, **6**, 13416–13420.
45 A. C. Riches, J. G. Sharp, D. B. Thomas and S. V. Smith, *J. Physiol.*, 1973, **228**, 279–284.
46 Y. Yan, Y. Wang, J. K. Heath, E. C. Nice and F. Caruso, *Adv. Mater.*, 2011, **23**, 3916–3921.
47 H. K. Kleinman, M. L. McGarvey, L. a Liotta, P. G. Robey, K. Tryggvason and G. R. Martin, *Biochemistry*, 1982, **21**, 6188–6193.
48 H. K. Kleinman, M. L. McGarvey, J. R. Hassell, V. L. Star, F. B. Cannon, G. W. Laurie and G. R. Martin, *Biochemistry*, 1986, **25**, 312–318.
49 H. K. Kleinman and G. R. Martin, *Semin. Cancer Biol.*, 2005, **15**, 378–386.
50 M. Van Beek, L. Jones and H. Sheardown, *Biomaterials*, 2008, **29**, 780–9.
51 G. Kogan, L. Soltes, R. Stern and P. Gemeiner, *Biotechnol. Lett.*, 2006, **29**, 17–25.
52 Y. Geng, P. Dalhaimer, S. Cai, R. Tsai, M. Tewari, T. Minko and D. E. Discher, *Nat. Nanotechnol.*, 2007, **2**, 249–255.
53 M. Björnmalm, M. Faria, X. Chen, J. Cui and F. Caruso, *Langmuir*, 2016, **32**, 10995–11001.
54 M. Björnmalm, M. Faria and F. Caruso, *J. Am. Chem. Soc.*, 2016, **138**, 13449–13456.
55 S. N. Bhatia and D. E. Ingber, *Nat. Biotechnol.*, 2014, **32**, 760–772.
56 E. W. Esch, A. Bahinski and D. Huh, *Nat. Rev. Drug Discov.*, 2015, **14**, 248–260.

Table of Contents entry

A simple and modular flow-based system is used to rapidly screen fundamental interactions of soft polymer particles with biologically relevant microenvironments under flow-conditions.

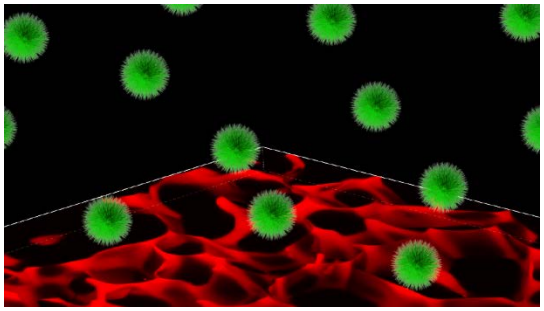

Author/s:
Braunger, JA; Bjornmalm, M; Isles, NA; Cui, J; Henderson, TMA; O'Connor, AJ; Caruso, F

Title:
Interactions between circulating nanoengineered polymer particles and extracellular matrix components in vitro

Date:
2017-02-01

Citation:
Braunger, J. A., Bjornmalm, M., Isles, N. A., Cui, J., Henderson, T. M. A., O'Connor, A. J. & Caruso, F. (2017). Interactions between circulating nanoengineered polymer particles and extracellular matrix components in vitro. BIOMATERIALS SCIENCE, 5 (2), pp.267-273. https://doi.org/10.1039/c6bm00726k.